Nonholonomic Dynamic Rolling Control of Reconfigurable 5R Closed Kinematic Chain Robot with Passive Joints

Tasuku YAMAWAKI, Osamu MORI and Toru OMATA
Department of Precision Machinery Systems
Tokyo Institute of Technology
4259 Nagatsuta, Midoriku, Yokohama, Kanagawa, Japan
{m0130yamawaki, mori, omata}@pms.titech.ac.jp

Abstract **We have developed a self-reconfigurable robot which can form a 5R closed kinematic chain, only two of whose joints are actuated. This paper discusses its dynamic rolling. When it rolls, it has one DOF of its absolute orientation besides two DOFs of its shape. We show that the absolute orientation is subject to an acceleration constraint, not a velocity constraint. Therefore, the dynamics of the rolling motion needs to be formulated to control it. This paper proposes a controller which can reduce its negative acceleration caused by gravity. The shape and orientation of the robot cannot be controlled simultaneously. This paper proposes a control strategy switching shape and orientation controllers. We verify the effectiveness of the control strategy by simulations and experiments.**

1 Introduction

The purpose of this study is to develop a simple but useful robot. Such a robot is less expensive and more reliable than complex robots. A group of such robots could do more than a single complex robot.

As an example, we have developed a self-reconfigurable robot which can form 5R and 4R closed kinematic chains as shown in Fig. 1 by coupling the same two 2R open kinematic chains whose first joints are unactuated [1]. Fig. 2 shows a photo of the robot forming the 5R closed kinematic chain. We have proposed coupling of limbs with a passive joint(s) to form a parallel robot with the same number of actuators as its degrees of freedom (DOFs). Both the 5R and 4R closed kinematic chains can be used as a parallel robot with the same number of actuators as its DOFs. Our previous experiments reveal that the 5R closed kinematic chain can locomote by rolling as shown in Fig. 1 (B') [2]

Rolling motions of closed kinematic chains have been studied. Matsuo et al [4] studied learning of the rolling motion of a 6R closed kinematic chain using Genetic Algorithm. Yim et al [5] has developed a reconfigurable robot, which can form a closed kinematic chain. All joints of these robots are actuated. Lee and Sanderson[6] have developed the "Tetrobot" and studied its dynamic rolling motion.

In general a rolling motion is considered as the sequence of phases as shown in Fig. 3. In (A) a robot gains an initial velocity for rolling. In (B) through (D) it rolls about a point on the floor and in (E) it lands on the floor. It bounds on the floor in general as shown in (F), which can trigger the next step of rolling by saving some energy. Lee and Sanderson studied dynamic control to tip the Tetrobot for transition from (A) to (B) and to restore its shape in the phase of rolling about a point, (B) through (D). They also simulate the impact in the phase (E).

In this paper, we discuss dynamic rolling control of our 5R closed kinematic chain robot (*5R closed robot* or just *robot* for simplicity) in the phases of rolling about a point (B) through (D) and (F)) by focusing on its nonholonomic property. We show that the rolling velocity of the 5R closed robot can be accelerated/ decelerated even in these phases. Therefore the 5R closed robot can roll starting with a lower initial velocity.

The 5R closed robot has one DOF of its absolute orientation besides two DOFs of its shape. The absolute orientation is independent of the constraint for forming the closed kinematic chain. If its unactuated joints were actuated, the closed kinematic chain would be over-actuated but the absolute orientation could not be driven directly. Section 2 derives dynamic equations of motion and shows that the absolute orientation is subject to a second-order nonholonomic constraint. Since it is not subject to a velocity constraint, the dynamics of the rolling motion needs to be formulated to control it.

The shape and orientation of the robot cannot be controlled simultaneously. Section 3 proposes a control strategy switching shape and orientation controllers. Sections 4 and 5 show simulation and experimental results and the effectiveness of the proposed control strategy.

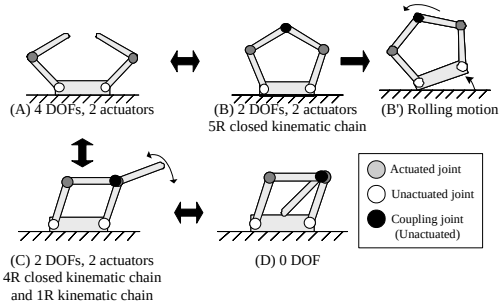

Figure 1: Self-reconfigurable robot by coupling

Figure 2: Our self-reconfigurable robot forming a 5R closed kinematic chain

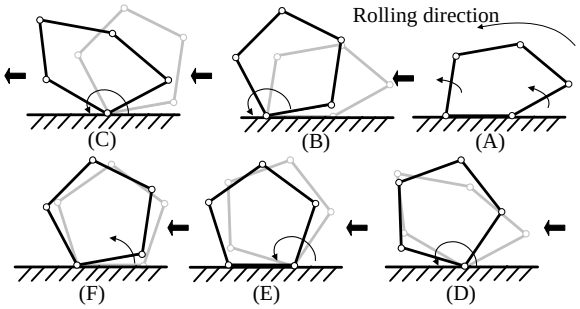

Figure 3: Phases of rolling motion

2 Dynamics for rolling motion

In the rolling motion, the orientation of this 5R closed kinematic chain can be classified into five cases as shown in Fig. 4 (A) to (E) according to the arrangement of actuators. If (E) is seen from the back of the sheet, the arrangement of actuators is seen as (E'), which is equivalent to (A). Therefore, their dynamic equations of motion are the same, while the rotation direction of (E) is opposite to that of (A). Similarly, (B) and (D) can be described as the same equations of motion. Therefore, we deal with only (A), (C) and (D).

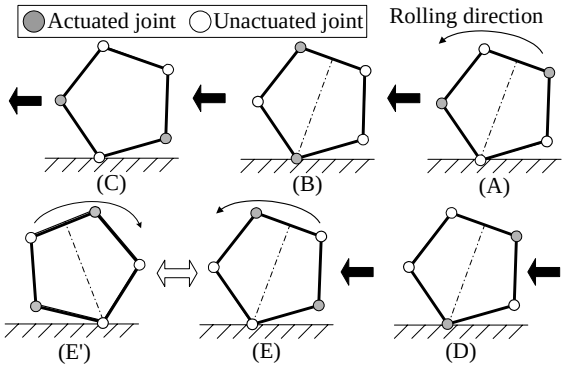

Figure 4: Arrangements of the actuators

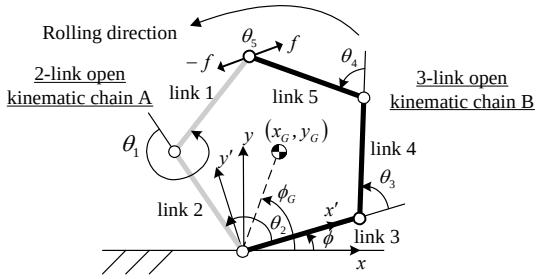

Figure 5: Common model of the rolling motion

Fig. 5 shows a common model for (A), (C) and (D). Let link3 be the link whose one end is leaving the floor and ϕ be its orientation angle from the floor. The joint angles θ_1 through θ_4 are defined as shown in the figure. Define generalized coordinates as $\mathbf{q} = (\theta_1\ \theta_2\ \theta_3\ \theta_4\ \phi)^T$. Corresponding to $\mathbf{q}$, the joint torque vector $\boldsymbol{\tau}$ is given by

$$\text{case (A)} \quad \boldsymbol{\tau} = (\tau_1\ 0\ 0\ \tau_4\ 0)^T \quad (1)$$
$$\text{case (C)} \quad \boldsymbol{\tau} = (\tau_1\ 0\ \tau_3\ 0\ 0)^T \quad (2)$$
$$\text{case (D)} \quad \boldsymbol{\tau} = (0\ \tau_2\ 0\ \tau_4\ 0)^T \quad (3)$$

Let (x_G, y_G) be the center of the gravity (COG) of the 5R closed kinematic chain and ϕ_G be the angle between the floor and COG, which we call the "COG angle". When $\phi_G < 90$ [deg], the angular velocity of the COG $\dot{\phi}_G$ is decelerated by gravity. If ϕ_G can reach $\phi_G > 90$ [deg], $\dot{\phi}_G$ is accelerated by gravity. The aim of this control for rolling is that $\phi_G > 90$ [deg]. Therefore ϕ_G is controlled actually instead of ϕ in Section 3.

This 5R closed kinematic chain is modeled as two open kinematic chains; one is the 2-link open kinematic chain 'A', consisting of links 1 and 2, the other is the 3-link open kinematic chain 'B', consisting of links 3 through 5. They are coupled at their end-points with the unactuated coupling joint θ_5. The constraint for forming the closed kinematic chain can be written with respect to the local coordinate system $x'y'$ attached to link 3 as

$$x' = l_1 c_{12} + l_2 c_2 = l_3 + l_5 c_{34} + l_4 c_3, \quad (4)$$
$$y' = l_1 s_{12} + l_2 s_2 = l_3 + l_5 s_{34} + l_4 s_3, \quad (5)$$

where s and c stand for sin and cos, and $s_{ij} = \sin(\theta_i + \theta_j)$ etc., and l_i is the length of the ith link. We have the velocity constraint by taking the time derivative of Eqs. (4) and (5):

$$J_A \begin{pmatrix} \dot{\theta}_1 \\ \dot{\theta}_2 \end{pmatrix} = J_B \begin{pmatrix} \dot{\theta}_3 \\ \dot{\theta}_4 \end{pmatrix}. \quad (6)$$

The column vectors of $J_A \in R^{2\times 2}$ and $J_B \in R^{2\times 3}$, $\mathbf{j}_{Ai}$ and $\mathbf{j}_{Bi}$, are written as

$$\mathbf{j}_{A1}=\begin{pmatrix}-l_1 s_{12}\\ l_1 c_{12}\end{pmatrix},\quad \mathbf{j}_{A2}=\begin{pmatrix}-l_1 s_{12}-l_2 s_2\\ l_1 c_{12}+l_2 c_2\end{pmatrix},$$
$$\mathbf{j}_{B1}=\begin{pmatrix}-l_5 s_{34}-l_4 s_3\\ l_5 c_{34}+l_4 c_3\end{pmatrix}\ \text{and}\ \ \mathbf{j}_{B2}=\begin{pmatrix}-l_5 s_{34}\\ l_5 c_{34}\end{pmatrix}.$$

In Eq. (6), two variables from $\dot{\theta}_1$ through $\dot{\theta}_4$ can be selected as independent variables, since the number of the constraint equations is two. If its unactuated joints were actuated, the 5R closed kinematic chain would be over-actuated but ϕ could not be driven directly, since ϕ is independent of the constraint, Eq. (6). ϕ is subject to an acceleration constraint as described later.

Eq. (6) can be rewritten as

$$\Psi\dot{\mathbf{q}}=\mathbf{0}\in R^2 \tag{7}$$

where $\Psi=(\mathbf{j}_{A1}\ \mathbf{j}_{A2}\ \mathbf{j}_{B1}\ \mathbf{j}_{B2}\ \mathbf{0})$. By using Ψ in Eq. (7), the dynamic equation of motion of the 5R can be obtained in terms of the generalized coordinates $\mathbf{q}$:

$$M(\mathbf{q})\ddot{\mathbf{q}}+\mathbf{C}(\mathbf{q},\dot{\mathbf{q}})+\mathbf{G}(\mathbf{q})=\boldsymbol{\tau}+\Psi^T\mathbf{f} \tag{8}$$

where $M(\mathbf{q})\in R^{5\times5}$ is the inertia matrix, $\mathbf{C}(\mathbf{q},\dot{\mathbf{q}})\in R^5$ is the term of centrifugal force, $\mathbf{G}(\mathbf{q})\in R^5$ is the gravitational term and $\mathbf{f}=(f_x\ f_y)$ is the constraint force acting on the end-points of the open kinematic chains A and B.

By examining the condition in the paper [6], we can prove that ϕ is subject to a second-order nonholonomic constraint. We chose ϕ and two joint angles from θ_1 to θ_4 as three independent variables in $\mathbf{q}$. The remaining two variables are dependent. Let $N\in R^{5\times3}$ be the matrix whose columns are the bases of the null space of Ψ and $\dot{\mathbf{p}}\in R^3$ be the vector consisting of the three independent variables. $\dot{\mathbf{q}}$ can be written as $\dot{\mathbf{q}}=N\dot{\mathbf{p}}$. Dot-multiplying both sides of Eq. (8) by N^T, we obtain

$$N^TM\left(N\ddot{\mathbf{p}}+\dot{N}\dot{\mathbf{p}}\right)+N^T(\mathbf{C}+\mathbf{G})=N^T\boldsymbol{\tau} \tag{9}$$

since $\Psi N=0\in R^{3\times3}$. Eq. (9) can be rewritten as

$$\tilde{M}\ddot{\mathbf{p}}+\tilde{\mathbf{C}}+\tilde{\mathbf{G}}=\tilde{\boldsymbol{\tau}} \tag{10}$$

where $N^TMN=\tilde{M}\in R^{3\times3}$, $N^TM\dot{N}\dot{\mathbf{p}}+N^T\mathbf{C}=\tilde{\mathbf{C}}\in R^3$, $N^T\mathbf{G}=\tilde{\mathbf{G}}\in R^3$ and $N^T\boldsymbol{\tau}=\tilde{\boldsymbol{\tau}}\in R^3$.

For instance, if $\dot{\theta}_1$ and $\dot{\theta}_4$ are chosen as independent variables, we have $\dot{\mathbf{p}}=(\dot{\theta}_1\ \dot{\theta}_4\ \dot{\phi})^T$ and

$$N^T=\begin{pmatrix}1 & * & * & 0 & 0\\ 0 & * & * & 1 & 0\\ 0 & 0 & 0 & 0 & 1\end{pmatrix}$$

where '*' denotes a certain real number. The third element of $\tilde{\boldsymbol{\tau}}$ is zero. So is it when other joint angles are chosen as independent variables. The third element of $\tilde{\mathbf{G}}$ is not constant. Therefore, the third equation is a second-order nonholonomic constraint [6]. Thus, ϕ is not subject to a velocity constraint.

3 Control design

3.1 Equations of motion including ϕ_G

We establish the dynamic equations of motion including ϕ_G. The COG of the system, (x_G,y_G), is given by

$$x_G=\frac{1}{m_0}\sum_{i=1}^{5}m_i x_i,\quad y_G=\frac{1}{m_0}\sum_{i=1}^{5}m_i y_i:\quad m_0=\sum_{i=1}^{5}m_i$$

where m_i is the mass of the i th link, x_i and y_i are the COG of the i th link. ϕ_G can be written as

$$\tan\phi_G=\frac{y_G}{x_G}. \tag{11}$$

Taking the time derivative of Eq. (11), we obtain

$$L(\mathbf{q})\ddot{\mathbf{q}}-\ddot{\phi}_G=-K(\mathbf{q},\dot{\mathbf{q}}) \tag{12}$$

where $L(\mathbf{q})\in R^{1\times5}$ and $K(\mathbf{q},\dot{\mathbf{q}})\in R$. Taking the time derivative of Eq. (7), we obtain the constraints for $\ddot{\mathbf{q}}$,

$$\Psi\ddot{\mathbf{q}}+\dot{\Psi}\dot{\mathbf{q}}=\mathbf{0}\in R^2 \tag{13}$$

The dynamic equations of motion can be obtained from Eqs. (8), (12) and (13),

$$\begin{pmatrix}M(\mathbf{q}) & 0 & \Psi^T\\ L(\mathbf{q}) & -1 & 0\\ \Psi & \mathbf{0} & 0\end{pmatrix}\begin{pmatrix}\ddot{\mathbf{q}}\\ \ddot{\phi}_G\\ -\mathbf{f}\end{pmatrix}=\begin{pmatrix}\boldsymbol{\tau}-C(\mathbf{q},\dot{\mathbf{q}})-G(\mathbf{q})\\ -K(\mathbf{q},\dot{\mathbf{q}})\\ -\dot{\Psi}\dot{\mathbf{q}}\end{pmatrix} \tag{14}$$

In Eq. (14), the number of the constraints is eight and the number of the variables is ten, which are $\ddot{\theta}_1$ through $\ddot{\theta}_4$, $\ddot{\phi}$, $\ddot{\phi}_G$, $\mathbf{f}$ and $\boldsymbol{\tau}$. We can control two of them.

3.2 COG control mode

The COG control mode can control $\ddot{\phi}_G$ and the acceleration of one of the joints. Consider the case of Fig. 4 (A), for instance, and compute the joint torques τ_1 and τ_4. In Eq. (14), we express the matrix of the left-hand side as

$$\begin{pmatrix}M(\mathbf{q}) & 0 & \Psi^T\\ L(\mathbf{q}) & -1 & 0\\ \Psi & \mathbf{0} & 0\end{pmatrix}=(\mathbf{w}_1\ \cdots\ \mathbf{w}_8),$$

where $\mathbf{w}_i$ is the i th column vector of the matrix in the left-hand side. If we control $\ddot{\theta}_2$, Eq. (14) can be rewritten as

$$(\mathbf{w}_1\ \mathbf{w}_3\ \mathbf{w}_4\ \mathbf{w}_5\ \mathbf{w}_7\ \mathbf{w}_8\ \mathbf{z}_1\ \mathbf{z}_4)(\ddot{\theta}_1\ \ddot{\theta}_3\ \ddot{\theta}_4\ \ddot{\phi}\ -f_x\ -f_y\ \tau_1\ \tau_4)^T$$
$$=-(\mathbf{w}_2\ \mathbf{w}_6)\begin{pmatrix}\ddot{\theta}_2\\ \ddot{\phi}_G\end{pmatrix}+\mathbf{h} \tag{15}$$

where $\mathbf{z}_1=(-1\ 0\ 0\ 0\ 0\ 0\ 0)^T$, $\mathbf{z}_2=(0\ 0\ 0\ -1\ 0\ 0\ 0)^T$ and

$$\mathbf{h}=\begin{pmatrix}\boldsymbol{\tau}-\mathbf{C}(\mathbf{q},\dot{\mathbf{q}})-\mathbf{G}(\mathbf{q})\\ -K(\mathbf{q},\dot{\mathbf{q}})\\ -\Psi\dot{\mathbf{q}}\end{pmatrix}.$$

To obtain the joint torques, we rewrite Eq. (15) as follows

$$\left(\ddot{\theta}_1\ \ddot{\theta}_3\ \ddot{\theta}_4\ \ddot{\phi}\ -f_x\ -f_x\ \tau_1\ \tau_4\right)^T=\hat{M}_G^{-1}\hat{\mathbf{C}}_G \qquad (16)$$

where

$$\hat{M}_G=\left(\mathbf{w}_1\ \mathbf{w}_3\ \mathbf{w}_4\ \mathbf{w}_5\ \mathbf{w}_7\ \mathbf{w}_8\ \mathbf{z}_1\ \mathbf{z}_4\right),\ \hat{C}_G=-\left(\mathbf{w}_2\ \mathbf{w}_6\right)\begin{pmatrix}\ddot{\theta}_2\\ \ddot{\phi}_G\end{pmatrix}+\mathbf{h}$$

and we also assume that $\hat{M}_G$ is non-singular. Section 4.3 discusses singularities of $\hat{M}_G$. $\ddot{\theta}_1$, $\ddot{\theta}_3$, $\ddot{\theta}_4$, $\ddot{\phi}$ and $\mathbf{f}$ are dependently determined by Eq. (16). Therefore the COG control mode cannot control the shape of the 5R closed kinematic chain which is determined by two of θ_1 through θ_4.

We discuss how to give a desired acceleration of $\ddot{\phi}_G$ for rolling. If ϕ_G is not controlled and the shape of the 5R closed robot is constant, $\dot{\phi}_G$ is decelerated by gravity and ϕ_G may not exceed 90 [deg]. Let the deceleration (negative acceleration) be $\ddot{\phi}_{grav}(<0)$. The COG control mode reduces the deceleration by setting the desired acceleration

$$\ddot{\phi}_G=\kappa\ddot{\phi}_{grav} \qquad 0<\kappa<1.0 \qquad (17)$$

Note: If $\kappa>1$ the COG mode decelerates $\dot{\phi}_G$ more than gravity alone. This is useful for the robot to descend a slope or to stop suddenly when it rolls about a point. If $\kappa<0$, the COG mode absolutely accelerates $\dot{\phi}_G$ under gravity. However there is a tradeoff between reducing κ and maintaining an initial shape of the robot as discussed next.

$\ddot{\phi}_{grav}$ can be obtained as follows. If the shape is constant, the 5R closed robot can be regarded as a rigid-body. From the moment equilibrium condition, we have

$$\left\{I_G+m_0\left({x_G}^2+{y_G}^2\right)\right\}\ddot{\phi}_{grav}=-m_0 g x_G$$

$$\ddot{\phi}_{grav}=-\frac{m_0 g x_G}{I_G+m_0\left({x_G}^2+{y_G}^2\right)} \qquad (18)$$

where I_G is the moment of inertia of the whole 5R closed robot, m_0 is its mass and g is the gravity acceleration.

The smaller κ is, the smaller the deceleration becomes, however if it is too small, the shape changes significantly. On the other hand, the bigger κ is, the more likely ϕ_G do not exceed 90 [deg]. In Section 4, we select an appropriate value of κ by simulation.

In the COG control mode, one of the joint angles can be controlled. The 5R closed robot can avoid singularities by controlling it as we discuss in Section 4.3.

3.3 Shape control mode

The shape control mode controls two of $\ddot{\theta}_1$ through $\ddot{\theta}_4$. If we chose $\ddot{\theta}_1$ and $\ddot{\theta}_4$, we can rewrite Eq. (14) by using $\mathbf{w}_i$,

$$\left(\mathbf{w}_2\ \mathbf{w}_3\ \mathbf{w}_5\ \mathbf{w}_6\ \mathbf{w}_7\ \mathbf{w}_8\ \mathbf{z}_1\ \mathbf{z}_4\right)\left(\ddot{\theta}_2\ \ddot{\theta}_3\ \ddot{\phi}\ \ddot{\phi}_G\ -f_x\ -f_y\ \tau_1\ \tau_4\right)^T$$
$$=-\left(\mathbf{w}_1\ \mathbf{w}_4\right)\begin{pmatrix}\ddot{\theta}_1\\ \ddot{\theta}_4\end{pmatrix}+\mathbf{h} \qquad (19)$$

We can also rewrite Eq. (17) as

$$\left(\ddot{\theta}_1\ \ddot{\theta}_3\ \ddot{\theta}_4\ \ddot{\phi}\ -f_x\ -f_x\ \tau_1\ \tau_4\right)^T=\hat{M}_S^{-1}\hat{\mathbf{C}}_S \qquad (20)$$

where

$$\hat{M}_S=\left(\mathbf{w}_2\ \mathbf{w}_3\ \mathbf{w}_5\ \mathbf{w}_6\ \mathbf{w}_7\ \mathbf{w}_8\ \mathbf{z}_1\ \mathbf{z}_4\right),\ \hat{C}_G=-\left(\mathbf{w}_1\ \mathbf{w}_4\right)\begin{pmatrix}\ddot{\theta}_1\\ \ddot{\theta}_4\end{pmatrix}+\mathbf{h}$$

and it is assumed that $\hat{M}_S$ is non-singular. Section 4.3 discusses the singularities of $\hat{M}_S$. The joint torques, τ_1 and τ_4, can be given by Eq. (20). Note that the shape control mode cannot control $\dot{\phi}_G$ which is dependently obtained from Eq. (20).

A PD controller is applied to control two joint angles.

$$\ddot{\theta}_i=K_p\left(\theta_{ri}-\theta_i\right)-K_d\dot{\theta}_i \qquad (21)$$

where θ_{ri} is a desired angle, and K_p and K_d are feedback gains.

3.4 Condition for switching control modes

The condition for switching the two control modes is as follows. When $\phi_G\le 90$ [deg], we apply the COG control mode to achieve $\phi_G>90$ [deg]. Once $\phi_G>90$ [deg] is achieved, the shape control mode is applied. Until the robot lands on the floor, the shape can be controlled. It is our future work to obtain the optimal landing shape to stop or continue rolling. After switching to the shape control mode, ϕ_G may be less than 90 [deg] again because it is not controlled in the shape control mode. A solution is to delay the timing of switching the control modes.

4 Simulations

4.1 Physical parameters and initial conditions

Table 1 shows the length of the i th link, l_i, the mass, m_i, the length to the center of gravity, l_{ci}, and the inertia moment, I_i. The initial conditions are $\theta_1=288$ [deg], $\theta_2=108$ [deg], $\theta_3=72$ [deg], $\theta_4=72$ [deg], $\phi=20$ [deg], $\dot{\theta}_1$ through $\dot{\theta}_4$ are 0 [deg/s], and $\dot{\phi}=\dot{\phi}_G=68$ [deg/s]. Suppose that θ_1 and θ_4 are actuated joints as shown in Fig. 4 (A). The COG control mode controls $\ddot{\phi}_G$ and $\ddot{\theta}_2$

whose desired acceleration is 0 [deg/s^2]. Changing κ as 1.0, 0.8 and 0.1, we observe ϕ_G and the shape of the 5R closed kinematic chain. The shape control mode control $\ddot{\theta}_1$ and $\ddot{\theta}_4$ whose desired angles are $\theta_1 = 288$ [deg] and $\theta_4 = 72$ [deg].

Table 1 Physical parameters of each link

l_1	0.25 m	m_1	1.01 kg	l_{c1}	0.125 m	I_1	7.8×10^{-3} kg m^2
l_2	0.25 m	m_2	1.37 kg	l_{c2}	0.175 m	I_2	9.7×10^{-3} kg m^2
l_3	0.25 m	m_3	0.94 kg	l_{c3}	0.125 m	I_3	1.8×10^{-2} kg m^2
l_4	0.25 m	m_4	1.37 kg	l_{c4}	0.175 m	I_4	9.7×10^{-3} kg m^2
l_5	0.25 m	m_5	0.97 kg	l_{c5}	0.097 m	I_5	1.7×10^{-2} kg m^2

4.2 Simulation results

Figs. 6 and 7 show simulation results of ϕ_G and the configurations of the 5R closed robot, respectively. The configurations after that pointed by "a" are controlled by the shape control mode. When $\kappa = 1.0$ in Fig. 6, ϕ_G cannot reach 90 [deg] and return toward zero by gravity. When $\kappa = 0.8$ and $\kappa = 0.1$, ϕ_G can reach 90 [deg] and is accelerated by gravity after $\phi_G > 90$. In this simulation, the closer to one κ is, the smaller the change in the shape is. For other arrangements of actuators in Fig. 4 (C) and (D), the same results are obtained, since their torques are calculated to obtain the same desired $\ddot{\phi}_G$.

4.3 Singularity

We examine singular configurations at which $\hat{M}_G$ and $\hat{M}_S$ become singular in the workspace. These matrices are functions of three independent variables, ϕ and two variables from θ_1 through θ_4, however it turns out that ϕ is independent of the singular configurations in this example. When θ_2 and θ_4 are chosen as the independent variables, Fig. 8 shows the singular configurations. In the area (c), the 5R closed robot cannot actually form the closed shape geometrically. The condition number of $\hat{M}_G$ is more than 200 in the areas (a) and (b), that of $\hat{M}_S$ is more than 200 in the area (b). We define these areas as singular configurations, since the observed torques in these areas exceed the maximum limits of our actuators.

The dashed-dotted line is the simulation result when $\kappa = 0.1$ corresponding to Fig. 7 (B). The COG control mode is switched to the shape control mode at the point indicated as "×". The robot avoids the singular area (a), although it is not intended.

Using Fig.8, the robot can intendedly avoid singular configurations even in the COG control mode. When θ_2 is increased by the PD controller, the trajectory of configurations indicated by the dashed line is farther from the singular area (a) than that by the dashed-dotted line.

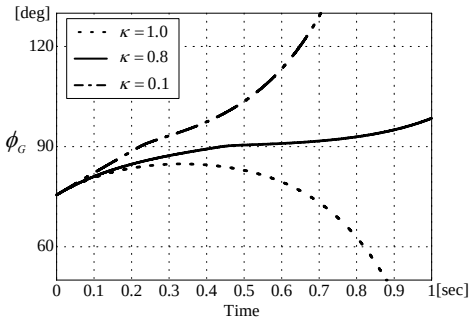

Figure 6: Angles of COG of the 5R closed kinematic chain

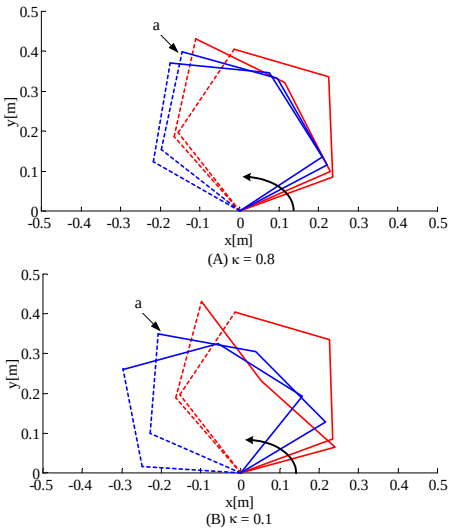

Figure 7: Simulation results

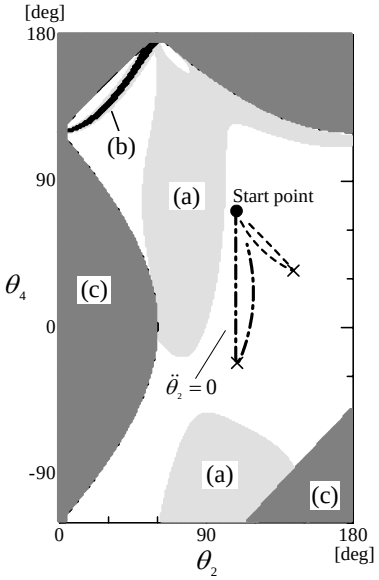

Figure 8: Singularities in the workspace of the simulation

5 Experiments

We conduct two experiments using the real robot in Fig. 2. The physical parameters of the robot have been shown in Table 1. In the first experiment, the switching control strategy proposed in Section 3.2 is applied with $\kappa = 0.8$. In the second experiment, only the shape control mode is used to maintain the initial shape of the robot. The two experiments are also conducted on a slope of 5 [deg].

The initial shape is $\theta_1 = 288$ [deg], $\theta_2 = 108$ [deg], $\theta_3 = 72$ [deg] and $\theta_4 = 72$ [deg]. θ_1 through θ_4 and $\dot{\theta}_1$ through $\dot{\theta}_4$ are measured by encoders, ϕ and $\dot{\phi}$ by a gyro sensor attached on link 3. ϕ_G and $\dot{\phi}_G$ are respectively obtained by Eq. (11) and taking the time derivative of Eq. (11).

Table 2 shows initial velocities of ϕ_G in these experiments. Fig. 9 shows the experimental results of ϕ_G. (A) shows that the robot can achieve $\phi_G > 90$ by the switching control strategy (snapshots are shown in Fig. 10), but cannot when only the shape control mode is applied. The same results are obtained on the slope as shown in (B).

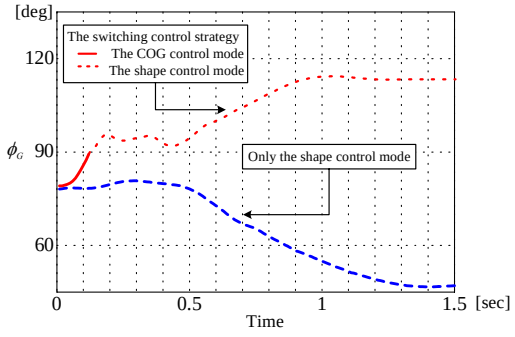

(A) On the flat surface

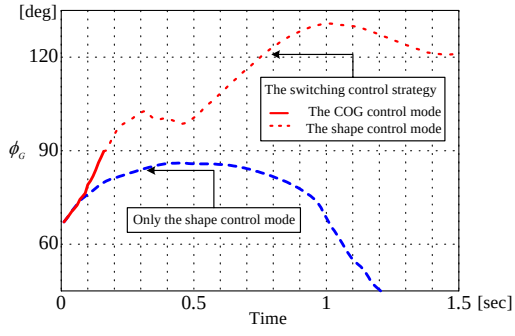

(B) On the slope

Figure 9: Experimental results

Table 2 Initial conditions

	Only the shape control mode	The switching control strategy
$\dot{\phi}_G$ on a flat surface	22.25 [deg/s]	21.21 [deg/s]
$\dot{\phi}_G$ on the slope	92.78 [deg/s]	89.02 [deg/s]

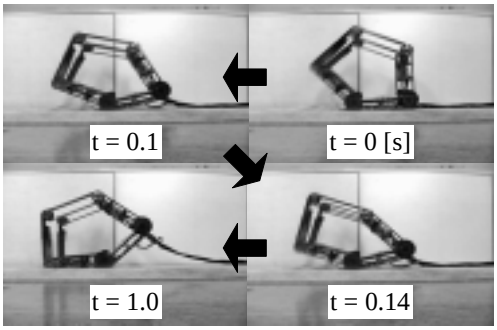

Figure 10: Snapshots of the rolling motion

6 Conclusion

For the dynamic rolling motion of the 5R closed kinematic chain robot, this paper has focused on its nonholonomic property and proposed a control strategy switching the two control modes: the COG control mode and the shape control mode. The COG control mode can reduce the negative acceleration caused by gravity which acts on the robot when it rolls about a point on the floor.

This robot we developed is self-reconfigurable. Since it can locomote by rolling when its shape is the 5R closed kinematic chain, it is useful if it can perform manipulative tasks after locomotion. The 5R closed kinematic chain can be used as a parallel manipulator and the 4R closed kinematic chain as shown in Fig. 1 may also be useful to perform some tasks. It is our future work to conduct experiments of manipulation.

Reference

[1] O. Mori and T. Omata, “Coupling of Two 2-Link Robots with a Passive Jointfor Reconfigurable Planar Parallel Robot”, Proc. of the IEEE Int. Conf. on Robotics and Automation, pp. 4120-4125, 2002.

[2] O. Mori, T. Yamawaki and T. Omata, “Control of Self-Reconfigurable Parallel Robot by Coupling Open Kinematic Chains with Unactuated Joints,” SICE Annual Conference 2002 CD-ROM, WM06-4, 2002.

[3] Y. Matsuo and V. Ampornaramveth, “A Wheel-Shaped Multi-Actuator System as a Test Bed for Autonomous Decentralized Motion Control,” Trans. IEEE of Japan, 117-C(12), pp. 1840-1847, 1997.

[4] M. Yim, Y. Zhang and D. Duff : ”Modular Robots,” IEEE SPECTRUM, vol. 39, no. 2, pp. 30-34, The institute of Electrical and Electronics Engineers, 2002.

[5] W. H. Lee and A. C. Sanderson: “Dynamic Rolling Locomotion and Control of Modular Robots”, IEEE Trans. on Robotics and Automation, vol. 18, no. 1, pp. 32-41, 2002.

[6] G. Oriolo and Y. Nakamura: “Control of Mechanical Systems with Second-Order Nonholonomic Constraints: Underactuated Manipulators,” Proceedings of the 30th Conference on Decision and Control, pp.2398-2403, 1991.